Water-hydrogen-polaron coupling at anatase TiO_2(101) surfaces: a hybrid Density Functional Theory study

Ya-Nan Zhu[1,2], Gilberto Teobaldi[3,4,5], Li-Min Liu[2*]

[1]Beijing Computational Science Research Center, Beijing 100193, China

[2]School of Physics, Beihang University, Beijing 100191, China.

[3]Scientific Computing Department, STFC UKRI, Rutherford Appleton Laboratory, Harwell Campus, OX11 0QX Didcot, United Kingdom

[4]Stephenson Institute for Renewable Energy, Department of Chemistry, University of Liverpool, L69 3BX Liverpool, United Kingdom

[5]School of Chemistry, University of Southampton, Highfield, SO17 1BJ Southampton, United Kingdom

Email: liminliu@buaa.edu.cn

Abstract: Defects and water generally co-exist on the surfaces of reducible metal oxides for heterogeneous photo-catalysis in aqueous environments, which makes quantification and understanding of their coupling essential for development of practical solutions. To this end, here we explore and quantify the coupling between water (H_2O) and hydrogen (H) induced electron-polarons on the TiO_2 anatase (101) surface by means of first-principles simulations. In the absence of H_2O, the hydrogen-induced electron-polaron localizes preferentially around the energetically favored sub-surface H site. Its hopping barrier to neighboring sites in the sub-surface is about 0.29 eV. Conversely, following H_2O adsorption, surface trapping of the electron-polaron becomes energetically favored, and the diffusion barrier from sub-surface to surface decreases by 0.15 eV. H_2O adsorption is shown to be effective also in decreasing the proton diffusion energy barrier within the same layer by reducing the polaron-proton coupling, and promoting diffusion towards the sub-surface in line with recent experimental observation on water-dispersed anatase TiO_2 nanoparticles [Nat Commun 2018, 9, 2752].

1. Introduction

Since Fujishima and Honda first discovered the decomposition of water on TiO_2 electrode under ultraviolet light in 1972,[1] TiO_2 has become one of the most widely used photo-catalysts. Defects are inevitably present in TiO_2 samples due to the synthesis procedure, and known to drive the physical and chemical properties of the substrate. The role of defects, such as oxygen vacancies, Ti interstitials and hydroxyls for the surface reactivity of TiO_2 has been extensively studied.[2-10] Excess electrons donated by such defects can interact with lattice phonons to form (electron) polarons, which in turn may affect the system's charge carriers mobility as well as its chemical reactivity[8, 11-19]. Understanding the formation and properties of polarons in TiO_2 is therefore crucial for rational design of high-performance photo-catalysts based on this material.

Recently, extensive theoretical and experimental research has been devoted to the behavior of polarons in transition metal oxides, especially on TiO_2. The formation and stability of polarons in anatase and rutile TiO_2 have been widely discussed. [3, 6, 20-33] Several computational studies have suggested that polarons in rutile are more stable than that in anatase, with the details of the simulation protocol e.g. standard vs. hybrid Density Functional Theory (DFT) being critical for the results of the simulations. [21-24] Setvin et al[21] suggested that the excess electrons in rutile prefer to form a small polaron, localized at any Ti atom, and that such small polarons can hop between neighboring sites. In contrast, Scanning Tunneling Microscopy (STM) and Spectroscopy (STS) results supported by DFT simulations indicate that excess electrons in anatase are found to prefer a free-carrier state, and can only be trapped near oxygen vacancies. Perhaps unsurprisingly, Spreafico et al.[22] found that the calculated stability of polarons in TiO_2 is sensitive to the amount of Hartree-Fock exchange. On the basis of random phase approximation (RPA) calculations using PBE0 functional with 30% Hartree-Fock exchange, it was found that excess electrons can form stable polarons in anatase too, in the absence of any defect.

The defects donated excess electrons can transfer from one site to another in TiO_2, thus affecting the chemical reactivity.[25] Kowalski et al found that the excess electrons induced by the oxygen vacancy in rutile TiO_2 preferentially stay at the second sub-surface layer. However, first-principles molecular dynamics (FPMD) simulations indicate that they can also fluctuate from surface sites to the third sub-surface layer.[27] Reticcioli et al. found that polaron trapping in the bulk is energetically less favorable than on surface and sub-surface sites, and that the polaron can easily hop from sub-

surface to surface. The same authors also suggested that the distribution of polarons could affect the stability of TiO_2 surfaces based on first-principles calculations and experimental surface characterization techniques.[33] DFT+U simulations by Selcuk and Selloni indicate that the distribution of excess electrons is strongly affected by the exposed anatase surface, its environment and the nature of the electron donor.[25]

As the precise distribution of polarons between the surface and sub-surface region is expected to strongly affect surface reactions, the interaction between polarons and adsorbates has attracted wide interest. [34-38] DFT+U results by Deskins et al.[34] suggest that charge transfer from the reduced surface to the adsorbate occurs when the electronegativity of the adsorbate is larger than the surface electronegativity. Reticcioli et al.[35] found that the CO adsorption on the rutile TiO_2 (110) can induce polaron diffusion from the sub-surface to surface region because of favorable polaron-CO interactions. By interplay between STM measurements and DFT calculations, Yim, et al.[38] suggested that water adsorption could also affect the distribution of polarons. Specifically, they found that surface adsorbed water and methanol can attract excess electrons to the surface due to energetically favorable coupling between adsorbates and polarons.

Water (H_2O) is invariably present on the TiO_2 surface in non ultra-high vacuum condition, and it is known to dissociate into one hydroxyl (OH) and one hydrogen atom (H) at ambient conditions.[39] The hydrogen atom can diffuse from the surface to the sub-surface.[10, 40] Meanwhile the introduction of the hydrogen can also introduce excess electrons and, potentially, polarons in the system, which could affect light absorption properties by the corresponding gap states.[41] TiO_2 hydrogenation under high H_2 pressure leads to formation of solar-light absorbing black TiO_2.[42] Using a combination of in-situ Transmission Electron Microscopy (TEM) and DFT calculations, Lu et al suggested that hydrogen treatment of TiO_2 leads to accumulation of hydrogen into the sub-surface region. They found that a thin nanoscale layer of amorphous hydroxylated TiO_2 forms at the beginning of the photocatalysis in water environment, which greatly affects H_2 production.[40] Although, these results clearly indicate that the distribution of hydrogen in TiO_2 samples play a vital role for the catalytic reactivity of the substrate, the details of the interactions between hydrogen contamination and excess electrons in TiO_2 are fare from established in the currently available literature.

Motivated by these considerations, and the lack of previous results on the matter,[34-38] here we quantify, by first principles simulations, the mutual effects that hydrogen-induced polarons and adsorbed water molecules exert on one another at anatase (101) surfaces, with special attention to the energetically favored trapping site of both the hydrogen contamination and the polaron as well as their diffusion barriers. In the first part of the paper, we investigate the dependence of the polaron distribution on the surface or sub-surface adsorption of hydrogen. The changes in atomic and electronic structure induced by the polaron are characterized and discussed in detail. In the second

part of the paper, we quantify and discuss the coupling between the hydrogen-induced polaron and water adsorption together with its role in affecting both the energetically favored polaron distribution and diffusion of hydrogen in the system.

2. Computational methods

The DFT calculations were carried out using the CP2K package,[43] that describes electrons' wave functions by a hybrid Gaussian and plane wave approach. The cutoff of the plane wave was 280 Ry. To investigate the properties of polaron in anatase TiO_2 (101) surface, and following earlier results by Spreafico et al.[22], we used the PBE0 hybrid functional[44, 45] with 30% Hartree-Fock exchange. The Goedecker-Teter-Hutter (GTH) pseudopotentials[46] were used to describe the core electrons. The wavefunctions of the valence electrons were expanded using the optimized double-zeta polarized basis sets (m-DZVP).[47] The auxiliary density matrix method (ADMM)[48] was employed to reduce the cost of simulations. As discussed in the specialist literature, excess electrons in anatase tend to be localized at small concentration,[22] as predicted by RPA. In Ref. [22], 30% Hartree-Fock exchange was used to obtain stable polarons.[22] The anatase TiO_2 (101) surface was modeled using four tri-layers following Ref. 25 with (1×4) (10.36 Å ×15.06 Å) surface supercells. A vacuum-buffer of 12 Å is used to separate replicated images of the slab along the non-periodic direction perpendicular to the plane of the slab. The structures were fully relaxed with a SCF convergence of 2×10^{-7} Hartree.

To calculate the polaron transfer energy, the polaron hopping mechanism based on the Marcus/Emin-Holstein-Austion-Mott (EHAM) theory was employed.[49-53] In this approach, the electronic states are described in form of parabolic energy surfaces. The transition state is the cross point of the energy surfaces for the initial states and final states. A linear interpolation scheme[54] was used to fit potential energy surfaces and quantify the energy barrier for polaron hopping between adjacent (Ti) sites. Energy barriers for proton diffusion were computed using the climbing-image nudged elastic band (CI-NEB)[55] method as implemented in CP2K with a spring constant of 0.2 eV $Å^{-2}$.

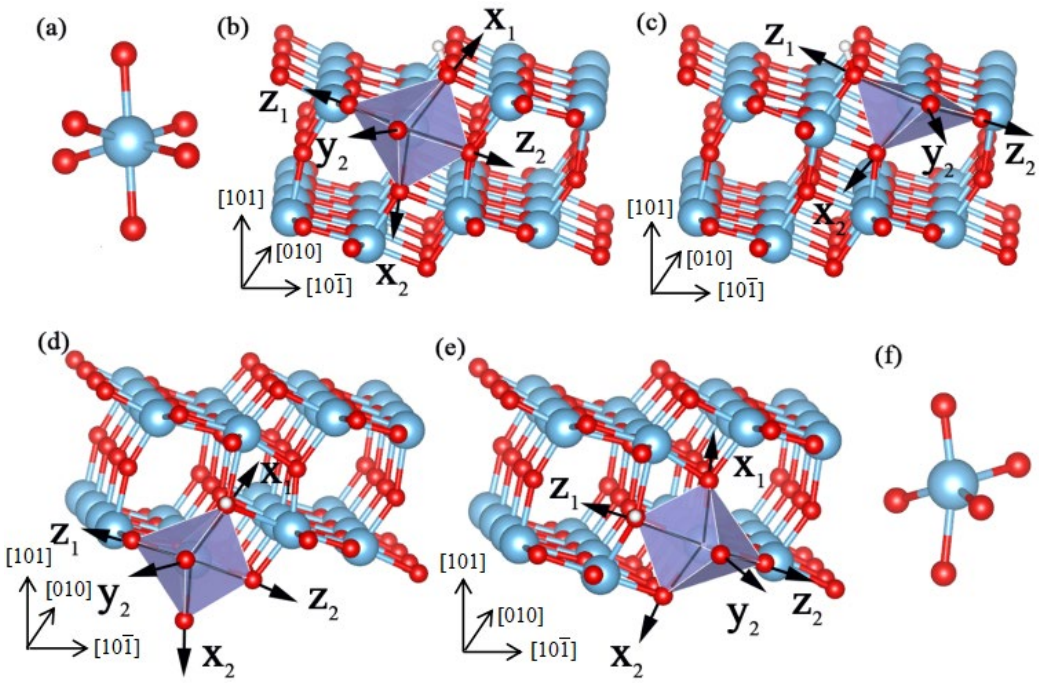

Figure 1. The atomic structure and crystallographic directions of the anatase (101) surface in the presence of surface and sub-surface H adsorption. (a) Schematic model of the TiO_6 unit. (b) The sur-6c site for the polaron induced by a surface adsorbed hydrogen. (c) The polaron sur-5c site for surface hydrogen. (d) The sub-1 site for sub-surface hydrogen. (e) The sub-2 site for sub-surface hydrogen. (f) Schematic model of the TiO_5 unit. The blue, red and white balls represent Ti, O and H atoms, respectively. The purple octahedrons show the calculated the crystal fields for the given Ti ion. The y_i and z_i axes (i=1,2) run parallel to the (101) slab-plane. Conversely, the x_i axes are perpendicular to the slab-plane.

3. Results and discussion

3.1. Polaron induced changes in the octahedral crystal field

In order to investigate how the H adsorption affects the catalytic properties of transition metal oxides, the anatase TiO_2(101) surface is taken as model system. The anatase (101) surface present two kinds of surface oxygen atoms with two- and three-fold coordination (Fig 1b and c). The adsorption sites for H have been previously investigated.[9, 10] When H is adsorbed on the surface, the polaron induced by the H typically prefers to stay at the surface rather than at the sub-surface region. On the surface, the polaron can trap either at the five- fold coordinated (sur-5c) or the six-fold

coordinated (sur-6c) site.

When the H is adsorbed at the sub-surface. The polaron introduced by the sub-surface H typically sits at three sites in the surface (sur-6c) and sub-surface (sub-1, sub-2), as shown in Fig. 1. The relative and adsorption energy of each considered site is listed in Table 1. Our simulations indicate that H prefers to adsorb on the surface rather than at the sub-surface by about 0.41 eV, which is in agreement with previous work.[9, 10] For surface H, the energy of the sur-5c or sur-6c are nearly degenerate to within 10 meV. Thus, the simulations indicate that the polaron on the surface can nearly equivalently sit on the sur-5c or sur-6c site. For the sub-surface H, the polaron prefers to stay in the sub-surface rather than on the surface by about 0.16 eV.

Table 1. Comparison of the calculated energy for the considered systems with surface and sub-surface H-adsorption as a function of the polaron trapping site. Same labeling as in Fig. 1. The energy of the most stable structure is set to zero. ($E_{relative} = E - E_{stable}$. $E_{adsorption} = E - E_{perfect} - 1/2E_{H_2}$.)

	H-surface		H-sub-surface		
	sur-5c	sur-6c	sub-1	sub-2	sur-6c
$E_{relative}$ (eV)	0.01	0	0.44	0.41	0.57
$E_{adsorption}$ (eV)	-0.31	-0.32	0.12	0.09	0.25

Next, we analyze how the polaron affects the crystal structure for the different systems considered. As mentioned above, the polaron can nearly equivalently sit at either the sur-5c or sur-6c site for the energetically favored surface adsorption of H. When the polaron is trapped at the sur-6c site, its Ti-atom is reduced from a pristine Ti^{4+} state into a Ti^{3+} one. As shown in Fig. 1 and Table 2, the x_1 vector marks the Ti-O bond towards the surface, whereas the x_2 vector represents the Ti-O bond towards the sub-surface. The x_1 bond is obviously shorter than the x_2 one because of the surface relaxation, which compresses inter-layer distances (also known as "surface effect"). The x_1 vector of the Ti atom in the sur-6c site is elongated from 1.823 Å to 2.106 Å because of Jahn-Teller effect (JT), while the y_2 and z_1 ones are increased by 0.1 Å. The other bond vectors of the Ti atom at the sur-6c do not change substantially. As shown in Fig. 2, the orbital occupied by the polaron corresponds to the $3d_{xz}$. When the polaron stays at the sur-5c site, the z_1 vector of the octahedral field centered on the sur-5c Ti-atom is increased from 1.804 Å to 2.015 Å, and the x_2 axis is elongated from 1.753 Å

to 1.935 Å. The changes on the other bonds change are minimal.

As for the sub-surface H adsorption, there are three possible sites for the polaron to trap. One is the sur-6c site, similar to the surface case. The other two, sub-1 and and sub-2 in Table 1 and Fig. 1, are just beneath the oxygen atom bound to the sub-surface H. We refer the the sub-surface Ti-atom closest to the surface Ti as sub-1. The other is referred to as sub-2. When the polaron stays at the sub-1 site, the main changes are induced on the x_1 Ti-O bond, which is elongated by about 0.2 Å. If the polaron lies at the sub-2 site, the length of the z_1 Ti-O bond is also increased by about 0.2 Å. When the polaron stays at the sur-6c site, the main change is along the x_2 vector, again with an extension of about 0.2 Å. As shown in Fig.2, we calculate the polaron to have t_{2g} character, in accordance with crystal field theory for local octahedral coordination. These results indicate that although the H-adsorption induced polaron can sit at several different sites, the bond elongation and structural relaxation are determined by the trapping site of the polaron rather than the adsorption site for the H-atom.

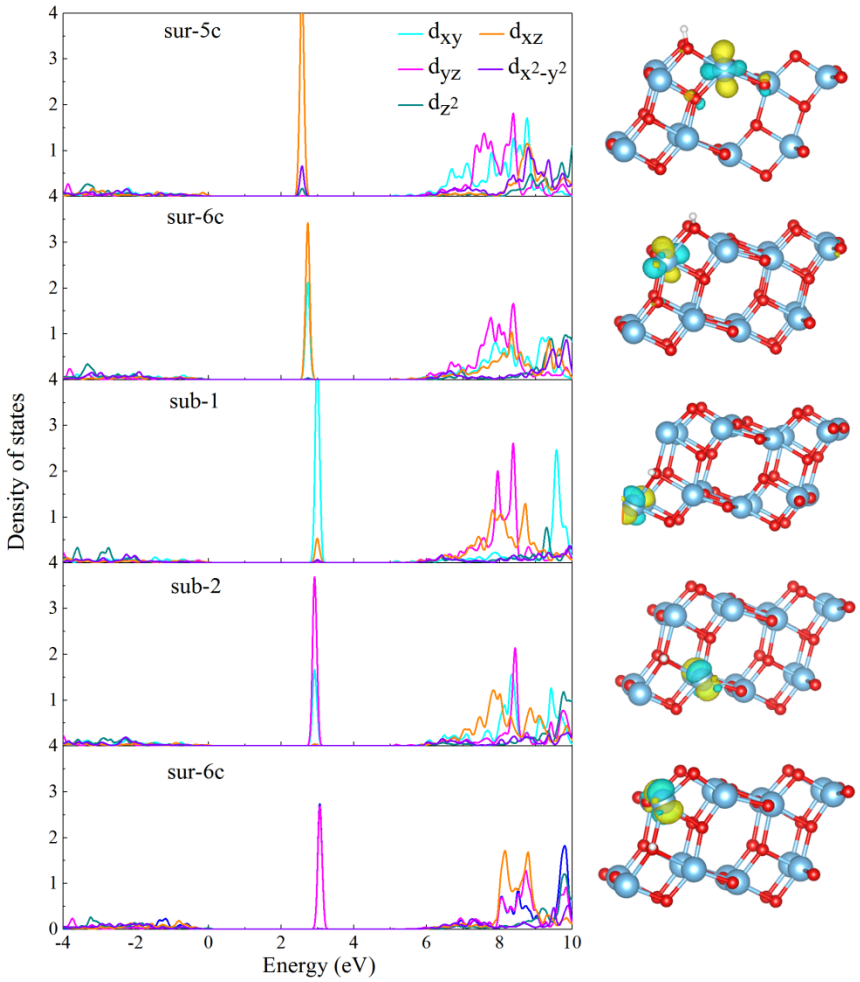

Figure 2. The calculated Ti^{3+} 3d orbital-resolved DOS (left) and corresponding real-space distribution of the polaron spin-density (right) for the different polaron trapping sites in the presence of both surface and sub-surface hydrogen adsorption. The isosurface for the spin density is 0.08 [a.u.].

Table 2. The calculated bond lengths (Å) around the Ti ion for the perfect hydrogen-free anatase (101) surface (P), and following hydrogen-induced polaron formation, together with the corresponding 3d occupied orbitals (last row). H(x,y,$z_{1,2}$) indicate that the H-atom adsorbs along the (x,y,$z_{1,2}$) axis of the crystal field centered on the Ti^{3+} atom.

structure	sur-5c		sur-6c		sub-1		sub-2		sur-6c	
	P	H (z_1)	P	H (x_1)	P	H (x_1)	P	H (z_1)	P	H (x_2)
x_1	-	-	1.823	2.106	1.863	2.066	1.966	2.049	1.823	1.878
x_2	1.753	1.935	2.045	2.038	1.983	1.965	1.835	1.907	2.045	2.221
y_1	1.961	1.967	1.927	1.931	1.929	1.972	1.93	2.005	1.927	2.007
y_2	1.961	1.977	1.927	2.028	1.929	2.022	1.93	2.002	1.927	2.031
z_1	1.804	2.015	1.971	2.073	1.952	2.001	1.971	2.182	1.971	2.021
z_2	2.021	2.026	2.082	2.062	1.975	2.003	1.96	1.983	2.082	2.133
orbital	-	d_{xz}	-	d_{xz}	-	d_{xy}	-	d_{yz}	-	d_{yz}

3.2. The role of water adsorption for the polaron localization

In addition to the structural changes caused by localization of the polaron, its interaction with molecular adsorbates is also expected to play an important role for the system's photo-catalytic activity. Since TiO_2 is a promising substrate for decomposing water and photo-degradation of organic contaminants in waste water, understanding of the interactions between water and defect-induced polaron is essential for rational development in the field.

As previously found, the diffusion of hydrogen from surface to subsurface becomes much easier with the water adsorption on the surface.[40] In addition, thin hydroxylated layers of TiO_2 can be formed in the real photo-catalysis processes. These layers have been shown to be critical for the production of H_2.[40] Previous work has also shown that adsorbates can change the distribution and properties of polarons because of the

physical coupling between the adsorbates and the polarons.[34-38] In spite of these published results, the coupling between adsorbed water and the polarons due to hydrogen contamination, and the role of such coupling for the trapping and diffusion of both protons and polarons, remain unquantified. To contribute to this knowledge gap, in the following we disentangle and quantify the water-hydrogen-polaron coupling at anatase TiO_2(101) surfaces, together with its role for polaron/proton trapping and diffusion.

We start analyzing, the role of water adsorption for the localization of hydrogen-induced polarons. The results in Table 1 for the (101) surface in the absence of adsorbed H_2O indicate that the polaron prefers to trap at the sub-surface region in the presence of sub-surface H-atoms (sub-2 site). This polaron-localization geometry is about 0.16 eV more stable than the one at the surface (sur-6c). Conversely, when a H_2O molecule adsorbs over the sur-5c Ti-site, the energy-favored site for polaron-trapping changes from the original sub-2 to sur-5c (Table 3), being sur-5c favored by 0.02 eV over sub-2. These results indicates that the H_2O adsorption can change the distribution of the polaron. More importantly, the polaron moves from the sub-surface to the surface. The novelty of these results stem from the fact that, although evidence of adsorbate-induced changes in the polaron distribution have been previously reported in Refs. [34-38], these studies focused predominantly on excess electrons induced by oxygen vacancies or interstitial Ti-atoms, neglecting hydrogen contamination and related excess electrons (polarons).

As shown in Table S2 in the Supporting Information, the calculated water-induce inversion in the relative energy of the polaron trapped at the sur-5c site with respect to sub-2 localization is, not unexpectedly, sensitive to the amount of Hartree-Fock exchange (HFX) included in the simulations. Reduction of HFX from 30% to 25% leads to the sub-2 polaron trapping site remaining favored by 30 meV over the sur-5c one even in the presence of H_2O, in contrast with the 30% HFX result. However, the 25% HFX sub-2/sur-5c energy difference is nevertheless by a factor of over five with respect to the analogous difference for the bare surface (from 0.16 eV, Table S1, to 0.03 eV, Table S2). These results indicate that the main qualitative conclusion of the manuscript remains valid regardless of the amount of HFX included in the simulations: by changing the relative trapping energies, H_2O adsorption can alter the distribution of H-induced polarons in anatase TiO_2(101).

To understand why water adsorption changes the energy-favored distribution of the polaron, we analyze the atomic structure of the systems under study before and after water adsorption (Fig. 3). The initial bond angle of O-Ti-O for the sur-5c site in the polaron and adsorbate free surface is about 164.96°. When the polaron localizes at the sur-5c site, the bond angle increases to 168.72° because of the previously mentioned elongation of the Ti-O by 0.2 Å (Table 2). Similarly to polaron trapping, also water adsorption increases the bond angle to 174.61° with parallel ~0.1 Å elongation of the

Ti-O bond opposite to the H_2O molecule. Thus, both polaron trapping and water adsorption help to release the effect of surface strain, contributing to partial recovery of the perfect octahedral crystal field for the Ti-atom at the sur-5c site. When both the polaron and water sits at the sur-5c site, the O-Ti-O angle becomes 178.51°. Overall these results demonstrate that the coupling between water adsorption and polaron trapping is effective in turning the underlying TiO_6 unit into a nearly prefect octahedral crystal field, reducing the strain energy.

Table 3. Comparison of the calculated energies for the considered systems with sub-surface H-adsorption as a function of the polaron trapping site after water adsorption of water on the surface.

site	sub-1	sub-2	sur-5c	sur-6c
$E_{relative}$ (eV)	0.07	0.02	0.00	0.25
$E_{adsorption}$ (eV)	0.15	0.10	0.08	0.33

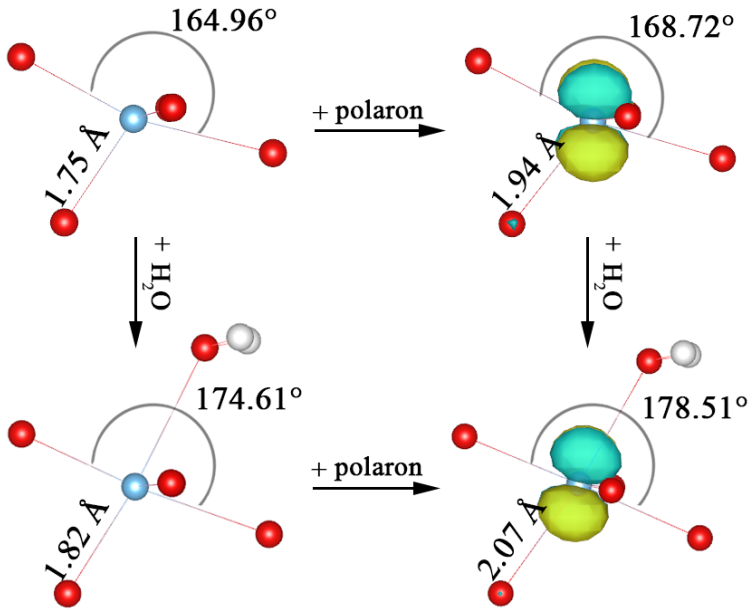

Figure 3. Schematic diagram of the H_2O-induced structural changes before and after the polaron localization at sur-5c. The isosurface for the polaron spin densities (right panels) is 0.12 [a.u.].

As first step towards inclusion of solvation effects in the simulations, we modeled also adsorption of 1 mono-layer (ML) H_2O (8 molecules). These simulations reveals further details of the role of H_2O adsorption in altering the relative energies of polaron trapping at anatase. As shown in the Supporting Information (Table S2), for 1 ML H_2O coverage polaron trapping at the sub-2 site is about 0.05 eV more stable than at the sur-5c one. Although in qualitative contrast with the 1/8 ML results (sur-5c favored over sub-2 by 0.02 eV), the 0.05 eV energy difference for 1 ML is *three times smaller* than what calculated in the absence of H_2O adsorption (Table 1 and Table S2: sub-2 sites favored by 0.15 eV over sur-5c). These observations reiterates the main point of the manuscript: by changing the relative trapping energies, H_2O adsorption can alter the distribution of H-induced polarons in anatase TiO_2(101).

To further investigate the effects of water adsorption on the polaron properties, we extended our study by considering also polaron hopping among the four typical (101) trapping sites, namely sur-6c, sur-5c, sub-1, and sub-2. Fig. 4(a) reports the possible transfer pathways we considered both in the presence and in the absence of adsorbed water. The energy favored paths are displayed in Fig. 4 (c).

The lower energy of the structures with sub-surface polaron trapping with respect to those with surface polaron localization in the absence of H_2O adsorption (Table 1) indicates a clear tendency for the polaron to diffuse from the surface to the sub-surface region. As shown in Fig.4, the energy barrier from sur-6c to the sub-1 is about 0.33 eV, and that of reverse process is about 0.46 eV. The energy barrier from sur-6c to sub-2 is about 0.38 eV, and the one from sub-2 to sur-6c is 0.54 eV. The energy barrier from sur-5c to sub-2 is 0.27 eV, while that from sub-2 to sur-5c is 0.42 eV. These results clearly indicate that, in the absence of H_2O adsorption, diffusion of the polaron from the surface to the sub-surface is energetically favored. The (over 0.12 eV) larger diffusion barriers for the inverse process, suggest that, once transferred, the polaron should remain in the sub-surface region, especially at room temperature. The nearly identical energies and lower diffusion energy barriers between different structures with the polaron trapped in the same layer (sur-6c/sur-5c and sub-1/sub-2 in Fig. 4(d) suggest that the polaron could transfer forth and reverse in the same layer.

Next, we quantify the extent to which H_2O adsorption affects polaron diffusion. As previously discussed (Table 3), in the presence of H_2O, the sur-5c site is the energetically favored polaron trapping site. As shown in Fig. 4(d), the calculated hopping barriers from sur-6c to sur-5c becomes 0.11 eV, which is about 0.21 eV smaller than the one without water adsorption. In addition, the adsorption of water changes the energy-favored polaron-transfer direction between sur-6c and sur-5c. Moreover, the energy of sur-5c becomes lower than that of sub-2. Thus, water adsorption induces polaron transfer from the sub-2 to the sur-5c site, promoting its diffusion from the sub-

surface to the surface with a relatively low energy barrier of 0.27 eV. The other transfer pathways do not change significantly in the presence of H_2O adsorption.

The reversal of the relative energies between initial state and final state for the polaron diffusion, together with the smaller barriers, altogether suggest that the water adsorption promote the diffusion of the polaron transfers towards sur-5c. These results demonstrate that H_2O adsorption can change the distribution of hydrogen-induced polarons in anatase (101) surfaces. Fig. 4(c) shows the lowest-barrier path of the polaron from the sub-surface to the surface in the presence of water: following hops between the sub-1 and sub-2 sites, the polaron eventually transitions from sub-2 to sur-5c.

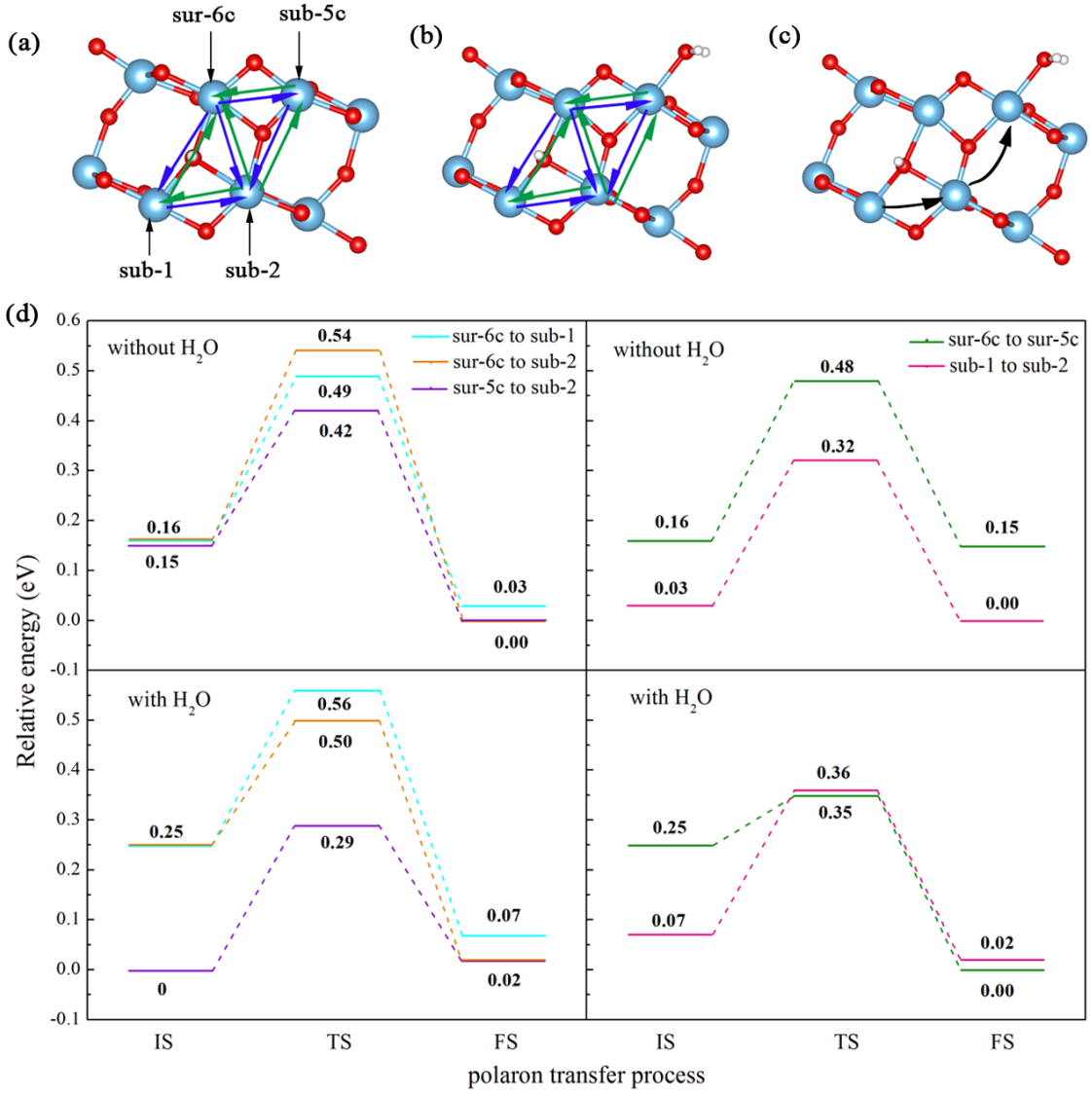

Figure 4. (a) The calculated polaron-hopping pathways without water. (b) The

calculated polaron-hopping pathways in the presence of adsorbed water. (c) The lowest-barrier diffusion path of the polaron from sub-surface to surface in the presence of adsorbed water. Panel (d) reports the calculated energy barriers for the hopping processed displayed in (a) and (b). For clarity, inter (left) and intra (right) processes have been separated.

As discussed above (Tables 1 and 3), for sub-surface H adsorption, H_2O adsorption changes the preferred polaron trapping site from the sub-surface to the surface region. Here, we discuss the coupling between the polaron and the proton (H) diffusion. Different proton transfer processes were considered with the hydrogen in the sub-surface, and the polaron in either the surface or sub-surface region. The proton transfer barriers between adjacent sites were modeled without and with water adsorption, and the calculated results are shown in Fig. 5.

Firstly, when the polaron stays around the hydrogen at sub-2 without water adsorption, the calculated proton diffusion barrier is 0.96 eV (Fig. 5b). With a calculated barrier of 0.95 eV in the presence of H_2O (Fig.5d), the simulations indicate sub-surface H-diffusion to be effectively insensitive to water adsorption in the presence of sub-surface (sub-2) polaron localization. Notably, when the polaron becomes localized at sur-5c following water adsorption, the proton-transfer barrier becomes 0.82 eV (Fig. 5c), which is 0.13 eV smaller than that for the polaron trapped at sub-2 (Fig.5d).

These results clearly indicate that proton diffusion in anatase (101) is significantly affected by the distance between the proton and the polaron because of electrostatic interactions. Based on the calculated reduction of the diffusion barriers, it can be concluded that water adsorption helps to decrease the coupling between the polaron and proton. As a result of such decreased coupling, the proton has greater freedom and tendency to diffuse between the different sites at the sub-surface region. These insights enable rationalization of recent experimental observations that H_2O adsorption on anatase TiO_2 leads to diffusion of protons from the surface to the subsurface regions.[40] Based on the simulations presented, H_2O adsorption induces decupling of polarons and protons, altering the relative energy of different polaron and proton trapping sides as well the energy barriers for proton and polaron diffusion. These changes cooperatively lead to preferential diffusion of protons and polarons towards opposite sides of the TiO_2/H_2O interface, as observed in the experiments,[40] and needed for surface formation of molecular hydrogen (H_2) by polaron-fuelled reduction of protons in the system.

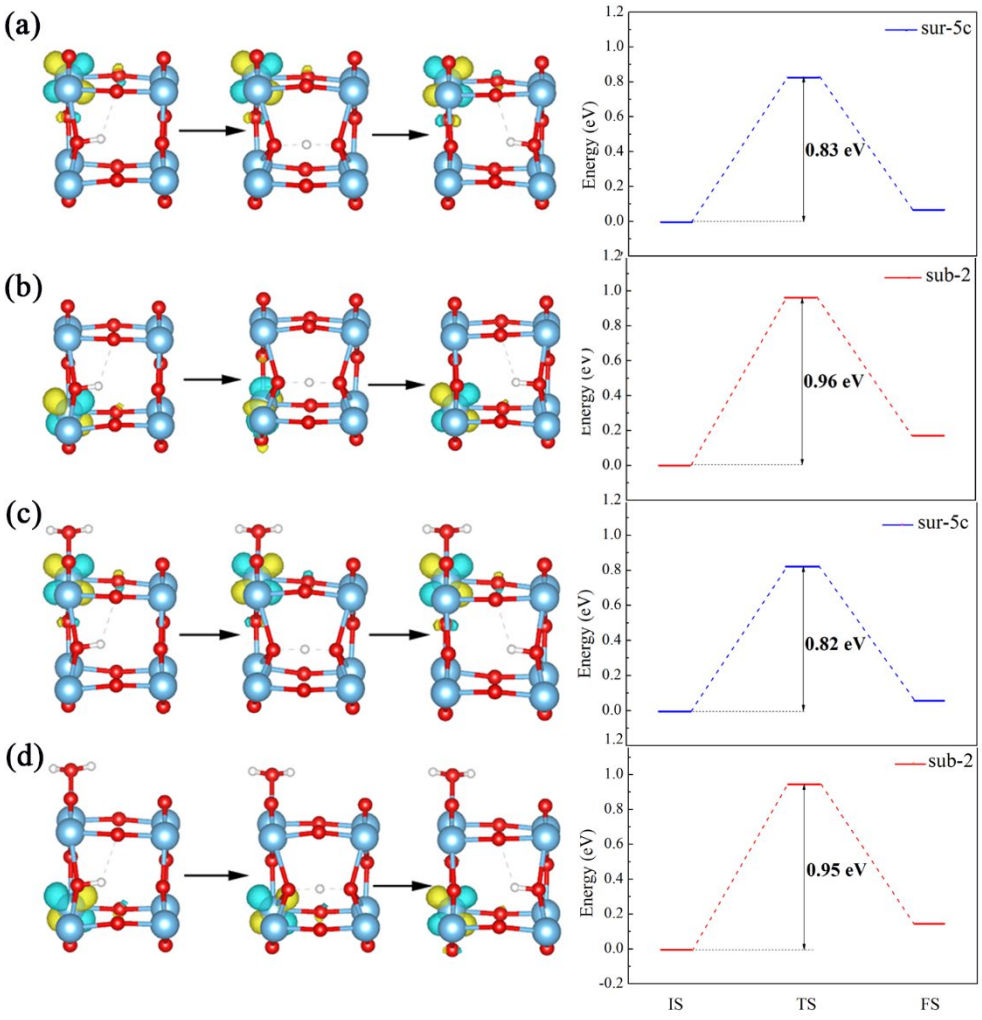

Figure 5. The transfer paths and related calculated barriers in the presence of sub-surface proton for different polaron localizations and H_2O adsorption: (a) sur-5c site, no H_2O; b) sub-2 site, no H_2O; c) sur-5c site, with H_2O; d) sub-2 site, with H_2O.

4. Summary and conclusions

In summary, we have quantified by first principles simulations the coupling between water and proton-induced polarons at the anatase (101) surface. Analysis of the results reveals that water adsorption not only affects the distribution of polarons, but it also favors decoupling between the polaron and proton, which should be vital for the production of molecular hydrogen (H_2) in water-based reaction environments. The energetically favored trapping site for the polaron is around the H atom in the absence

of water adsorption. Conversely, water adsorption attracts the polaron from the sub-surface to the surface region. Water induced decoupling of the polaron from the H site leads to enhanced diffusion of the proton within the layer. These results demonstrate that water adsorption does not only affect the distribution of H-induced polarons in anatase (101), but also diffusion processes for polarons and H-contamination.

Supporting Information:

Tests of the basis sets, the cutoff, the amount of Hartree-Fock exchange, the van der Waals correction and the water coverage.

Acknowledgement:

This work was supported by the National Natural Science Foundation of China (Grant No. 11974037, 51861130360 and U1930402), award of Tianhe-2JK computing time at the Beijing Computational Science Research Center (CSRC), and a Royal Society Newton Advanced Fellowships (grant No. NAF\R1\180242).

Reference

1. Fujishima, A.; Honda, K., Electrochemical Photolysis of Water at a Semiconductor Electrode. *Nature* 1972, 238, 37-38.

2. Cheng, H.; Selloni, A., Energetics and diffusion of intrinsic surface and sub-surface defects on anatase TiO_2 (101). *J. Chem. Phys.* 2009, 131, 054703.

3. Shibuya, T.; Yasuoka, K.; Mirbt, S. and Sanyal, B., A systematic study of polarons due to oxygen vacancy formation at the rutile TiO_2 (110) surface by GGA + U and HSE06 methods. *J. Phys.: Condens. Matter* 2012, 24, 435504.

4. Cheng, H.; Selloni, A., Surface and sub-surface oxygen vacancies in anatase TiO_2 and differences with rutile. *Phys. Rev. B* 2009, 79, 092101.

5. Janotti, A.; Varley, J. B.; Rinke, P.; Umezawa, N.; Kresse, G.; Van de Walle, C. G., Hybrid functional studies of the oxygen vacancy in TiO_2. *Phys. Rev. B* 2010, 81, 085212.

6. Morita, K.; Shibuya, T.; Yasuoka, K., Stability of Excess Electrons Introduced by Ti Interstitial in Rutile TiO_2(110) Surface. *J. Phys. Chem. C* 2017, 121, 3, 1602-1607.

7. Finazzi, E.; Di Valentin, C.; Pacchioni, G., Nature of Ti Interstitials in Reduced Bulk Anatase and Rutile TiO_2. *J. Phys. Chem. C* 2009, 113, 9, 3382-3385.

8. Papageorgiou, A. C.; Beglitis, N. S.; Pang, C. L.; Teobaldi, G.; Cabailh, G.; Chen, Q.; Fisher, A. J.; Hofer, W. A.; Thornton, G., Electron traps and their effect on the surface chemistry of TiO_2 (110). *PNAS* 2010, 107(6), 2391-2396.

9. Aschauer, U.; Selloni, A., Hydrogen interaction with the anatase TiO_2 (101) surface. *Phys. Chem. Chem. Phys.* 2012, 14(48), 16595-16602.

10. Islam, M. M.; Calatayud, M.; Pacchioni, G., Hydrogen Adsorption and Diffusion on the Anatase TiO_2 (101) Surface: A First-Principles Investigation. *J. Phy. Chem. C* 2011, 115, 14, 6809-6814.

11. Janotti, A.;Franchini, C.; Varley, J. B., Kresse, G.; Van de Walle, C. G., Dual behavior of excess electrons in rutile TiO_2. *Phys. Status Solidi RRL* 2013, 7, 199-203.

12. Yan, B.; Wan, D.; Chi, X.; Li, C.; Motapothula, M. R.; Hooda, S.; Yang, P.; Huang, Z.; Zeng, S.; Ramesh, A. G.; Pennycook, S. J.; Rusydi, A.; Ariando; Martin, J.; Venkatesan, T., Anatase TiO_2—A Model System for Large Polaron Transport. *ACS Appl. Mater. Interfaces* 2018, 10(44), 38201-38208.

13. Yan, L.; Chen, H., Migration of Holstein Polarons in Anatase TiO_2. *J. Chem. Theory Comput.* 2014, 10, 11, 4995-5001.

14. Moser, S.; Moreschini, L.; Jaćimović, J.; Barišić, O. S.; Berger, H.; Magrez, A.; Chang, Y. J.; Kim, K. S.; Bostwick, A.; Rotenberg, E.; Forró, L.; Grioni, M., Tunable polaronic conduction in anatase TiO_2. *Phys. Rev. Lett.* 2013, 110, 196403.

15. Di Valentin, C.; Selloni, A., Bulk and surface polarons in photoexcited anatase TiO_2. *J. Phys. Chem. Lett.* 2011, 2, 17, 2223-2228.

16. Deskins, N. A.; Rousseau, R.; Dupuis, M., Localized electronic states from surface hydroxyls and polarons in TiO_2(110). *J. Phys. Chem. C 2009, 113, 33, 14583-14586.*

17. Chiesa, M.; Paganini, M. C.; Giamello, E.; Murphy, D. M.; Di Valentin, C.; Pacchioni, G., Excess electrons stabilized on ionic oxide surfaces. *Acc. Chem. Res.* 2006, 39(11), 861-867.

18. Schneider, J.; Matsuoka, M.; Takeuchi, M.; Zhang, J.; Horiuchi, Y.; Anpo, M.; Bahnemann, D. W., Understanding TiO_2 photocatalysis: mechanisms and materials. *Chem. Rev.* 2014, 114(19), 9919-9986.

19. Setvin, M.; Aschauer, U.; Scheiber, P.; Li, Y.-F.; Hou, W.; Schmid, M.; Selloni, A.; Diebold, U., Reaction of O_2 with subsurface oxygen vacancies on TiO_2 anatase(101). *Science* 2013, 341, 6149, 988-991.

20. Reticcioli, M.; Diebold, U.; Kresse, G.; Franchini, C., (2019) Small Polarons in Transition Metal Oxides. In: Andreoni W., Yip S. (eds) *Handbook of Materials Modeling*. Springer, Cham.

21. Setvin, M.; Franchini, C.; Hao, X.; Schmid, M.; Janotti, A.; Kaltak, M.; Van de Walle, C. G.; Kresse, G.; Diebold, U., Direct view at excess electrons in TiO2 rutile and anatase. *Phys Rev Lett* 2014, 113(8), 086402.

22. Spreafico, C.; VandeVondele, J., The nature of excess electrons in anatase and rutile from hybrid

DFT and RPA. *Phys. Chem. Chem. Phys.* 2014, 16(47), 26144-26152.

23. Elmaslmane, A. R.; Watkins, M. B. and McKenna, K. P., First-Principles Modeling of Polaron Formation in TiO_2 Polymorphs. *J. Chem. Theory Comput.* 2018, 14, 7, 3740-3751.

24. Carey, J. J. and McKenna, K. P., Does Polaronic Self-Trapping Occur at Anatase TiO_2 Surfaces? *J. Phys. Chem. C,* 2018, 122, 27540-27553.

25. Selcuk, S. and Selloni, A., Facet-dependent trapping and dynamics of excess electrons at anatase TiO_2 surfaces and aqueous interfaces. *Nature Mater* 2016, 15, 1107–1112.

26. Yin, W.-J.; Wen, B.; Zhou, C.; Selloni, A.; Liu, L.-M., Excess electrons in reduced rutile and anatase TiO_2. *Surf. Sci. Rep.* 2018, 73, 58-82.

27. Kowalski, P. M.; Camellone, M. F.; Nair, N. N.; Meyer, B.; Marx, D., Charge localization dynamics induced by oxygen vacancies on the TiO_2 (110). *Phys. Rev. Lett.* 2010, 105, 146405.

28. Moses, P. G.; Janotti, A.; Franchini, C.; Kresse, G.; Van de Walle, C. G., Donor defects and small polarons on the TiO_2(110) surface. *J. Appl. Phys.* 2016, 119, 181503.

29. Morgan, B. J.; Watson, G. W., Intrinsic n-type Defect Formation in TiO_2: A Comparison of Rutile and Anatase from GGA+U Calculations. *J. Phys. Chem. C 2010,* 114(5), 2321-2328.

30. Morgan, B. J.; Watson, G. W. Polaronic trapping of electrons and holes by native defects in anatase TiO2. *Phys. Rev. B* 2009, 80(23).

31. Morgan, B. J.; Watson, G. W. A DFT+U description of oxygen vacancies at the TiO2 rutile (110) surface. *Surf. Sci.* 2007, 601(21), 5034-5041.

32. Chiesa, M.; Paganini, M. C.; Giamello, E.; Murphy, D. M.; Di Valentin, C.; Pacchioni, G., Excess electrons stabilized on ionic oxide surfaces. *Acc. Chem. Res.* 2006, 39(11), 861-867.

33. Reticcioli, M.; Setvin, M.; Hao, X.; Flauger, P.; Kresse, G.; Schmid, M.; Diebold, U. and Franchini, C., Polaron-Driven Surface Reconstructions. *Phys. Rev. X* 2017, 7, 031053.

34. Deskins, N. A.; Rousseau, R. and Dupuis, M., Defining the Role of Excess Electrons in the Surface Chemistry of TiO_2. *J. Phys. Chem. C* 2010, 114, 5891–5897.

35. Reticcioli, M.; Sokolović, I.; Schmid, M.; Diebold, U.; Setvin, M. and Franchini, C., Interplay between Adsorbates and Polarons CO on Rutile TiO_2 (101). *Phys. Rev. Lett.* 2019, 122, 016805.

36. Wen, B.; Yin, W.-J.; Selloni, A.; Liu, L.-M., Defects, Adsorbates, and Photoactivity of Rutile TiO_2 (110): Insight by First-Principles Calculations. *J. Phys. Chem. Lett.* 2018, 9, 18, 5281-5287.

37. Wang, R.; Fan, H., The location of excess electrons on H_2O/TiO_2(110) surface and its role in the surface reactions. *Mol. Phys.* 2017, 116:2, 171-178.

38. Yim, C. M.; Chen, J.; Zhang, Y.; Shaw, B.-J.; Pang, C. L.; Grinter, D. C.; Bluhm, H.; Salmeron, M.; Muryn, C. A.; Michaelides, A.; Thornton, G., Visualization of Water-Induced Surface Segregation of

Polarons on Rutile TiO_2(110). *J. Phys. Chem. Lett.* 2018, 9, 4865-4871.

39. Diebold, U., The surface science of titanium dioxide. *Surf. Sci. Rep.* 2003, 48, 53-229.

40. Lu, Y.; Yin, W.-J.; Peng, K.-L.; Wang, K.; Hu, Q.; Selloni, A.; Chen, F.-R.; Liu, L.-M.; Sui, M.-L., Self-hydrogenated shell promoting photocatalytic H_2 evolution on anatase TiO_2. *Nat Commun* 2018, 9, 2752.

41. Wen, B.; Hao, Q.; Yin, W.-J.; Zhang, L.; Wang, Z.; Wang, T.; Zhou, C.; Selloni, A.; Yang, X. and Liu, L.-M. Electronic structure and photoabsorption of Ti^{3+} ions in reduced anatase and rutile TiO_2. *Phys. Chem. Chem. Phys.*, 2018, 20, 17658-17665.

42. Chen, X.; Liu, L.; Yu, P. Y.; Mao, S. S., Increasing Solar Absorption for Photocatalysis with Black Hydrogenated Titanium Dioxide Nanocrystals. *Science* 2011, 331, 6018, 746-750.

43. VandeVondele, J.; Krack, M.; Mohamed, F.; Parrinello, M.; Chassaing, T.; Hutter, J., Quickstep: Fast and accurate density functional calculations using a mixed Gaussian and plane waves approach. *Comput. Phys. Commun.* 2005, 167, 2, 103-128.

44. Adamo, C.; Barone, V., Toward reliable density functional methods without adjustable parameters: The PBE0 model. *J. Chem. Phys.* 1998, 110, 6158.

45. Perdew, J. P.; Ernzerhof, M.; Burke, K., Rationale for mixing exact exchange with density functional approximations. *J. Chem. Phys* 1996, 105 (22), 8.

46. Goedecker, S.; Teter, M. and Hutter, J., Separable dual-space Gaussian pseudopotentials. *Phys. Rev. B* 1996, 54, 1703.

47. VandeVondele, J.; Hutter, J., Gaussian basis sets for accurate calculations on molecular systems in gas and condensed phases. *J. Chem. Phys.* 2007, 127(11), 114105.

48. Guidon, M.; Hutter, J.; VandeVondele, J., Auxiliary Density Matrix Methods for Hartree-Fock Exchange Calculations. *J. Chem. Theory Comput.* 2010, 6(8), 2348-2364.

49. Marcus, R. A.; Sutin, N., Electron transfers in chemistry and biology. *Biochim. Biophys. Acta* 1985, 811, 265-322.

50. Marcus, R. A., Electron transfer reactions in chemistry theory and experiment. *Rev. Mod. Phys.* 1993, 65, 599-610.

51. Emin, D.; Holstein, T., Studies of small-polaron motion IV. Adiabatic theory of the Hall effect. *Ann. Phys.* 1969, 53, 3, 439-520.

52. Holstein, T., Studies of Polaron Motion: Part I. The Molecular-Crystal Model. *Ann. Phys.* 2000, 281, 706-724.

53. Austin, I. G.; Mott, N. F., Polarons in crystalline and non-crystalline materials. *Adv. Phys.* 2010, 50, 7, 757-812.

54. Deskins, N. A.; Dupuis, M., Electron transport via polaron hopping in bulk TiO_2: A density functional theory characterization. *Phys. Rev. B* 2007, 75, 195212.

55. Henkelman, G.; Uberuaga, B. P., and Jónsson, H., A climbing image nudged elastic band method for finding saddle points and minimum energy paths. *J. Chem. Phys.* 2000, 113, 9901.

TOC graphic